Determination of respiration and photosynthesis fractionation factors for atmospheric dioxygen inferred from a vegetation-soil-atmosphere analog of the terrestrial biosphere in closed chambers

Clémence Paul[1], Clément Piel[2], Joana Sauze[2], Nicolas Pasquier[1], Frédéric Prié[1], Sébastien Devidal[2], Roxanne Jacob[1], Arnaud Dapoigny[1], Olivier Jossoud[1], Alexandru Milcu[2,3], Amaëlle Landais[1]

[1] Laboratoire des Sciences du Climat et de l'Environnement, LSCE/IPSL, CEA-CNRS-UVSQ, Université Paris-Saclay, 91191 Gif-sur-Yvette, France

[2]Ecotron Européen de Montpellier (UAR 3248), Univ Montpellier, Centre National de la Recherche Scientifique (CNRS), Campus Baillarguet, Montferrier-sur-Lez, France

[3]Centre d'Ecologie Fonctionnelle et Evolutive, Univ Montpellier, CNRS, Univ Paul Valéry, EPHE, IRD, Montpellier, France

Correspondence: Clémence Paul (clemence.paul@lsce.ipsl.fr)

Abstract

The isotopic composition of dioxygen in the atmosphere is a global tracer which depends on the biosphere flux of dioxygen toward and from the atmosphere (photosynthesis and respiration) as well as exchanges with the stratosphere. When measured in fossil air trapped in ice cores, the relative concentration of ^{16}O, ^{17}O and ^{18}O of O_2 can be used for several applications such as ice core dating and past global productivity reconstruction. However, there are still uncertainties about the accuracy of these tracers as they depend on the integrated isotopic discrimination of different biological processes of dioxygen production and uptake, for which we currently have very few independent estimates. Here we determined the respiration and photosynthesis fractionation factors for atmospheric dioxygen from experiments carried out in a replicated vegetation-soil-atmosphere analog of the terrestrial biosphere in closed chambers with growing *Festuca arundinacea*. The values for ^{18}O discrimination during soil respiration and dark respiration in leaves are equal to - 12.3 ± 1.7 ‰ and - 19.1 ± 2.4 ‰, respectively. In these closed biological chambers, we also found a value attributed to terrestrial photosynthetic isotopic discrimination equal to + 3.7 ± 1.3 ‰. This last estimate suggests that the contribution of terrestrial productivity in the Dole effect may have been underestimated in previous studies.

1. Introduction

The oxygen cycle represents one of the most important biogeochemical cycles on Earth as oxygen is the second most important gaseous component in the atmosphere. Oxygen is an essential component for life on Earth as it is consumed by all aerobic organisms through respiration and produced by autotrophic organisms through photosynthesis.

The analysis of the oxygen isotopic composition classically expressed as $\delta^{18}O$ and $\delta^{17}O$ of O_2 in air bubbles trapped in ice cores is currently used to provide information on the variations of the low latitude water cycle and the productivity of the biosphere during the Quaternary (Bender et al., 1994; Luz et al., 1999; Malaizé et al., 1999; Severinghaus et al., 2009; Blunier et al., 2002; Landais et al., 2010). $\delta^{18}O$ of O_2 is also a very useful proxy for ice core dating through the resemblance of its variations with the variations of precession or summer insolation in the northern hemisphere (Shackleton, 2000; Dreyfus et al., 2007). These tracers are however complex and their interpretation relies on the precise knowledge of the various fractionation factors in the oxygen cycle.

First, interpreting the relationship between $\delta^{18}O$ of O_2 (or $\delta^{18}O_{atm}$) variations in ice core air and the low latitude water cycle (e.g. Severinghaus et al., 2009; Landais et al., 2010; Seltzer et al., 2017) is still debated because of the multiple processes involved. Dole (1936) reported the relative atomic weight of oxygen in the air and water of Lake Michigan and gave as a measure of the $\delta^{18}O$ value between both of about 21 ‰. Barkan and Luz (2005) showed that $\delta^{18}O_{atm}$ is enriched compared to the $\delta^{18}O$ of water of the global ocean (taken here as the Vienna Standard Mean Ocean Water, VSMOW) with a value of 23.88 ‰.With the more recent values of Pack et al. (2017) of 24.15 ‰ and Wostbrock and Sharp (2021) of 24.05 ‰, we can envisage an enrichment of $\delta^{18}O_{atm}$ with respect to VSMOW of about ~ 24 ‰.This Dole effect is the result of several isotopic discriminations caused by biotic processes that enrich the $\delta^{18}O_{atm}$ relative to the oceanic values of water $\delta^{18}O$. First measurements have shown that the photosynthesis itself is not associated with a strong isotopic discrimination and produces oxygen with an isotopic composition which is close to the isotopic composition of the consumed water (Vinogradov et al., 1959; Stevens et al., 1975; Guy et al., 1993; Helman et al., 2005; Luz & Barkan, 2005). This is in contrast to the early results of Dole and Jenks (1959) who proposed a photosynthetic isotopic discrimination for plants and algae of 5‰. Vinogradov et al. (1959) challenged the results of Dole and Jenks (1944) by explaining that the ^{18}O enrichment of O_2 during their photosynthesis experiments is the result of contamination by atmospheric O_2 and respiration. Guy et al. (1993) studied the photosynthetic isotopic discrimination on spinach thylakoids, cyanobacteria (*Anacystis nidulans*) and diatoms (*Phaeodactylum tricornutum*) and found on average only a slight isotopic discrimination of

0.3‰ which they considered negligible. Luz and Barkan (2005) also corroborates this idea by studying photosynthetic isotopic discrimination on Philodendron and did not obtain a ^{18}O enrichment of the O_2 produced. This absence of isotopic discrimination can be theoretically explained by the process of O_2 generation within photosynthesis (photosystem II) involving water oxidation by the oxygen evolving complex (Tcherkez and Farquhar, 2007). For the oceanic biosphere, the isotopic composition of O_2 produced by photosynthesis is very close to the isotopic composition of the ocean. However, in terrestrial biosphere the $\delta^{18}O$ of water split during photosynthesis (leaf water) is highly variable both spatially and temporally because of the decrease of $\delta^{18}O$ of meteoric water toward higher latitudes (Dansgaard, 1974) and the enrichment in heavy isotopes in leaf water during evaporation (Dongmann et al., 1974). The mean $\delta^{18}O$ enrichment of leaf water isotopic composition has been estimated between + 4.5 and + 6 ‰ with respect to the isotopic composition of mean global ocean water (Bender et al., 1994; Hoffmann et al., 2004). On top of this enrichment, the terrestrial and oceanic Dole effects are mostly explained by the respiratory isotopic discrimination of the order of magnitude of + 18 ‰ (Bender et al., 1994).

Because of the isotopic enrichment in leaf water, the terrestrial Dole effect has been initially estimated to be 5 ‰ higher than the oceanic Dole effect and $\delta^{18}O_{atm}$ used to estimate changes in the balance between land and marine productivity (Wang et al., 2008; Bender et al., 1994; Hoffmann et al., 2004). However, the evidence by Eisenstadt et al. (2010) of isotopic discrimination up to + 6‰ for marine phytoplankton photosynthesis rather suggests that the marine and terrestrial Dole effects are of the same order of magnitude. More specifically, Eisenstadt et al. (2010) determined several photosynthetic isotopic discrimination values depending on the phytoplankton studied (*Phaeodactylum tricornutum* = 4.5 ‰, *Nannochloropsis sp*. = 3 ‰, *Emiliania huxleyi* = 5.5 ‰ and *Chlamydomonas reinhardtii* = 7 ‰). If marine and terrestrial Dole effects are similar, then the past variations of $\delta^{18}O_{atm}$ cannot be attributed to different proportions of terrestrial or marine Dole effects. They would be better related to low latitude water cycle influencing the leaf water $\delta^{18}O$ consumed by photosynthesis and then the $\delta^{18}O$ of O_2 produced by this process (with a larger flux in the low latitude vegetated regions). This is supported by orbital and millennial variations of $\delta^{18}O_{atm}$ in phase with calcite $\delta^{18}O$ in Chinese speleothem, a proxy strongly related to the intensity of hydrological cycle in South-East Asia (Severinghaus et al., 2009; Landais et al., 2010; Extier et al., 2018). The aforementioned studies show that qualitative and quantitative interpretation of $\delta^{18}O_{atm}$ relies strongly on the estimate of O_2 fractionation factors in the biological cycle but data to constrain the fractionation factors associated with respiration and photosynthesis for the different ecosystems are sparse.

In addition to the use of $\delta^{18}O_{atm}$, the combination of $\delta^{17}O$ and $\delta^{18}O$ of O_2 provides a way to quantify variations in past global productivity (Luz et al., 1999). This method relies on the fact that O_2-

fractionating processes in the stratosphere and within the biosphere lead to different relationships between $\delta^{17}O$ and $\delta^{18}O$ of O_2. Oxygen is fractionated in a mass-independent manner in the stratosphere producing approximately equal ^{17}O and ^{18}O enrichments (Luz et al., 1999). On the contrary, the biosphere fractionating processes are mass-dependent such that the ^{17}O enrichment is about half the ^{18}O enrichment relative to ^{16}O. We thus define a $\Delta^{17}O$ anomaly as:

$$\Delta^{17}O = \ln(1 + \delta^{17}O) - 0.516 \times \ln(1 + \delta^{18}O) \quad (1)$$

$\Delta^{17}O$ of O_2 is equal to 0 by definition in the present-day troposphere (the standard for isotopic composition of atmospheric oxygen is the present-day atmospheric value). $\Delta^{17}O$ of O_2 is negative in the stratosphere and increases in biosphere productivity leads to an increase of $\Delta^{17}O$ of O_2. As for the interpretation of $\delta^{18}O_{atm}$, the quantitative link between $\Delta^{17}O$ of O_2 and biosphere productivity depends on the exact fractionation factors associated with biosphere processes (Brandon et al., 2020).

Several studies have been conducted to estimate the fractionation factors during biosphere processes of O_2 production and consumption. These fractionation factors are then implemented in global modeling approaches involving the use of models of global vegetation and oceanic biosphere for interpretation of $\Delta^{17}O$ of O_2 and $\delta^{18}O_{atm}$ in term of environmental parameters (Landais et al., 2007; Blunier et al., 2012; Reutenauer et al., 2015; Brandon et al., 2020). Most of the fractionation factors used in these modeling approaches were obtained from studies conducted at the cell level: cyanobacterium (Helman et al., 2005), *E. coli* (Stolper et al., 2018), microalgae (Eisenstadt et al., 2010). In these studies, the underlying assumption is that the fractionation factor associated with O_2 measured at the cell level can be applied at the ecosystem scale. Yet, results from studies conducted at a larger scale, e.g. at the soil scale by Angert et al. (2001) found a global terrestrial respiratory $^{18}O/^{16}O$ of O_2 discrimination for soil microorganisms varying between - 12 ‰ and - 15 ‰. This is lower than the - 18 ‰ discrimination classically used for respiration, with diffusion in soil playing a role in addition to the biological respiration isotopic discrimination. Angert and Luz (2001) also showed using experiments on roots of Philodendron plants and wheat seedlings that the respiratory discrimination of a soil with roots is lower (about - 12‰) than the - 18‰ discrimination associated with dark respiration. This is due to the low O_2 concentration in roots whose presence favors a slower diffusion. Later, Angert et al. (2003) found an even larger spread of O_2 isotopic discrimination in soil and showed that temperate and boreal soils have higher isotopic discrimination, respectively - 17.8 ‰ and - 22.5 ‰.

It has been suggested that the strong discrimination observed for boreal and temperate soils is due to the involvement of the alternative oxidase pathway (AOX, Bendall and Bonner, 1971) in addition to the usual COX respiratory pathway. In the COX respiration pathway, present in the majority in plants, the cytochrome oxidase enzyme catalyzes the oxygen reduction reaction. In the AOX pathway, the oxidation of ubiquinol molecules is directly coupled to the reduction of oxygen. Guy et al. (2005) showed that, for green tissues, the respiratory discrimination of the AOX pathway is much higher (- 31‰) than the one of the COX pathway (- 21‰). Similarly, Ribas-Carbo et al. (1995) found a higher respiratory discrimination in phytoplankton that engage the AOX pathway (- 31 ‰) relative to bacteria that engage the COX pathway (- 24 ‰).

Other studies had attempted to investigate the different respiratory discriminations in the light (dark respiration, Mehler reaction and photorespiration). As during the light period, dark respiration can be inhibited (70 % inhibition found by Tcherkez et al. (2017) and Keenan et al. (2019)), so that the other O_2 consuming processes are important to consider. The Mehler reaction reduces oxygen to form a superoxide ion which is converted to hydrogen peroxide (H_2O_2) in photosystem I and then further converted to water (Mehler, 1951). Photorespiration is the result of the oxygenase activity of Rubisco (Sharkey, 1998). This enzyme can oxidize ribulose-1,5-bisphosphate with an oxygen molecule O_2. This reaction causes a loss of CO_2 incorporation, thus decreasing the photosynthetic yield (Bauwe et al., 2010). Guy et al. (1993) first found a photorespiratory discrimination of - 21.7 ‰ and a $^{18}O/^{16}O$ discrimination of - 15.3 ‰ for the Mehler reaction. Later, on a study performed on pea, Helman et al. (2005) found $^{18}O/^{16}O$ discriminations of - 21.3 ‰ and - 10.8 ‰ respectively for photorespiration and Mehler reaction.

The above presented state of the art shows contrasting results for the determination of fractionation factors for the different photosynthesis and O_2 uptake processes, thus underlining the importance of performing new measurements to correctly interpret global variations of the isotopic composition of oxygen. Moreover, because there may be a difference between the fractionation factors at the cell level and at a broader level as shown for dark respiration in soil, we will favor here an approach at the scale of a terrarium including plant and soil.

In this study we developed a simplified vegetation-soil-atmosphere analog of the terrestrial biosphere in closed chamber of 120 dm^3 with the aim of estimating the fractionation factors of atmospheric dioxygen due to soil respiration, plant respiration and photosynthesis. With this setup we carried out several experimental runs with soil only and soil with plants in order to estimate the isotopic discrimination of the different compartments and check values obtained at the cell level. The implications for our interpretation of the Dole effect are also discussed.

2.Material and Methods

2.1. Growth chamber and closed system

2.1.1. Plant growth and experimental setup

a)

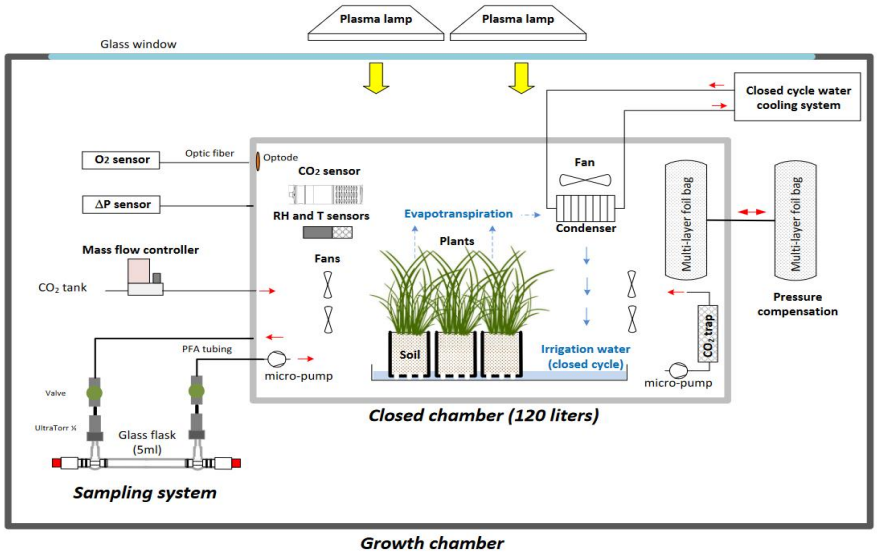

b)

Fig.1. A vegetation-soil-atmosphere analog of the terrestrial biosphere in a closed chamber. (a) Schematic of the closed chamber setup used for the terrestrial biosphere model. The 120 dm^3 gas tight closed chamber containing a terrestrial biosphere analogue is enclosed in a larger growth chamber from the Ecotron Microcosms platform. Main environmental parameters inside the closed

chamber are actively controlled and monitored: temperature (T), light intensity, CO_2, relative humidity (RH), pressure differential (ΔP). The water cycle in the closed chamber is shown in blue. **(b) Photograph of the closed chamber used in the experiment with *Festuca arundinacea*.**

Seeds of *Festuca arundinacea (Schreb.)*, also commonly called tall fescue, were first sown in a commercial potting soil (Terreau universel, Botanic, France. Composition: black and blond peat, wood fibre, green compost and vermicompost manure, organic and organo-mineral fertilizers and micronutrient fertilizers). During 15 to 20 days, they were then placed in a growth chamber of the Microcosms experimental platform of the European Ecotron of Montpellier (https://www.ecotron.cnrs.fr) under diurnal light-dark cycles (Table S1), air temperature set at 20 °C (T_{air}), air relative humidity (RH) at 80 % and CO_2 atmospheric concentration close to ambient air (concentration of CO_2 = 400 ppm).

Twelve pots (8 cm × 8 cm × 12 cm with 180 to 200 g of dry soil) containing approximately 25 to 30 mature fescue plants were used for each experimental run. All plants were placed in a plastic tray filled with tap water, inside an airtight transparent chamber manufactured from welded polycarbonate (10 mm wall thickness and 120 liters volume) similar to the chambers used by Milcu et al. (2013) (Fig. 1). The sealing of the closed chamber was checked before each experiment using helium.

To control temperature and light intensity inside the closed chamber, this smaller chamber was placed in a larger controlled environment growth chamber. Light was provided by two plasma lamps (GAVITA Pro 300 LEP02; GAVITA) with PAR = 200 $\mu mol \cdot m^{-2} \cdot s^{-1}$ and air temperature inside the closed chamber was regulated at 19 ± 1 °C by adjusting the growth chamber temperature.

The closed chamber (Fig. 1) was used as a closed gas exchange system with controlled, and continuously monitored, environmental parameters. Air and soil temperature (CTN 35, Carel), air relative humidity (PFmini72, Michell instrument, USA) and CO_2 atmospheric concentration (GMP343, Vaisala, Finland) were measured and recorded using the growth chamber datalogger (sampling rate = 1 min). O_2 concentration was continuously monitored using an optical sensor (Oxy1-SMA, Presens, Germany). Because precise O_2 concentration are determined in our samples by mass spectrometry (see next section), the measurements of the Oxy1-SMA were only used as a control during the experiment. The measured O_2 value for atmospheric air was adjusted to 20.9 % before each sequence of experiments and the same adjustment (offset) was then applied to the O_2 record during the following sequence.

Air relative humidity was regulated between 80 % and 90 % using a heat exchanger (acting as a condenser) connected to a closed cycle water cooling system. The condenser was positioned in a way to create a closed water cycle in the biological chamber (water vapor from evapotranspiration was condensed back into irrigation water). In order to keep the CO_2 mixing ratio close to 400 ppm during

the light periods, photosynthetic CO_2 uptake was compensated with injections of pure CO_2 using a mass flow controller (F200CV, Bronkhorst, The Netherlands). During the dark periods, a soda lime trap connected to a micro-pump (NMS 020B, KNF, Germany) was used to remove the excess CO_2 coming from respiration. CO_2 atmospheric concentration during the night was kept below 200 ppm.

To ensure atmospheric pressure stability in the closed chamber, a pressure compensation system, made of two connected 10 liters gas tight bags (Restek multi-layer polyvinyl fluoride foil gas sampling bag, USA), was installed. Each bag was half full of atmospheric air, the first one was installed in the closed chamber while the second one was outside this chamber. This way, each bag inflated or deflated in response to pressure variations caused either by O_2 or CO_2, uptake or release. The pressure difference between the closed chamber and the atmosphere was regularly measured using a differential sensor (FD A602-S1K Almemo, Ahlborn, Germany).

Finally, the enclosed air was mixed using and considered homogeneous seven brushless fans.

2.1.2. Gas sampling

To measure the isotopic composition along the experiment, small samples of gas were collected in 5 mL glass flasks, made of two Louwers H.V. glass valves (1-way bore 9mm Ref. LH10402008, Louwers Hanique, The Netherlands) welded together. Those flasks, previously evacuated, were mounted on PFA tubing ($1/4^{th}$) using two $1/4^{th}$ UltraTorr fitting (SS-4-UT-9, Swagelok, USA). Two manual valves (SS-4H, Swagelok, USA) were also installed on the PFA tubes to open or close the circuit. A micro-pump (NMS 20B, KNF, Germany) was finally turned on during air sampling to ensure closed chamber atmosphere circulation through the flask. The flow rate was equal to 1.6 L/min.

2.2. Isotopic measurements

2.2.1. Water extraction from leaf and isotopic analysis

After each experiment, the plant leaves were collected, placed in airtight flasks and immediately frozen at - 20°C for at least 24 hours to make sure there was minimal loss of water through vaporization when the vial was opened later. The extraction of water from leaves was done according to the procedure detailed in Alexandre et al. (2018). The vial was fixed onto a cryogenic extraction line and was first immersed in a liquid nitrogen Dewar to prevent any sublimation of the water. The water extraction line was emptied of most of its air ($< 10^{-5}$ Pa). Once this pressure was reached, the pump was turned off and a valve was closed in order to keep a constant static void within the system. The “reception” vial was then immerged in a liquid nitrogen Dewar which will act as a water trap whilst the sample vial for the water was then transferred to a water bath maintained at 75°C. The system was kept in these

conditions for no less than six hours, so that all the water present in the leaf and stems was extracted. Afterwards, in order to remove all of the organic compounds of the extracted water, an active charcoal was placed in the extracted water and left under agitation for the night.

For analysis of $\delta^{17}O$ and $\delta^{18}O$ of water, leaf water was converted to O_2 using a fluorination line for reaction of H_2O with CoF_3 heated to 370°C at LSCE. The isotopic composition of the dioxygen was measured an IRMS equipped with dual inlet (Thermo Scientific MAT253 mass spectrometer). The standard that was chosen was an O_2 standard calibrated against VSMOW. The precision was 0.015 ‰ for $\delta^{17}O$, 0.010 ‰ for $\delta^{18}O$ and 6 ppm for $\Delta^{17}O$ (Eq. (1)), for more details, refer to Landais et al. (2006).

The values of $\delta^{18}O$ and $\delta^{17}O$ of leaf water measured with respect to VSMOW are then expressed with respect to the isotopic composition of dioxygen in atmospheric air (classical standard for $\delta^{18}O$ and $\delta^{17}O$ of O_2 measurements). No consensus has been reached for the values of $\delta^{18}O$ and $\delta^{17}O$ of O_2 in atmospheric air with respect to $\delta^{17}O$ and $\delta^{18}O$ of H_2O of VSMOW. These differences are most probably to be attributed to the different analytical techniques used for preparing and measuring the samples (Yeung et al., 2018; Wostbrock et al., 2021). In our case, because we use a similar set-up with the one developed by Barkan and Luz (2003) for the analyses of the triple isotopic composition of O_2 in air (cf next section), we have chosen to base our calculation on their estimates. In this study, we have thus chosen the value of 23.88 ‰ for $\delta^{18}O$ of O_2 values with respect to VSMOW following (Barkan and Luz, 2005). As for the $\delta^{17}O$ of O_2 value with respect to VSMOW value, we use two different possible estimates from these authors, either 12.03 ‰ (Luz and Barkan, 2011) or 12.08 ‰ (Barkan and Luz, 2005). We acknowledge that because of the absence of consensus, slightly different values could be obtained for the fractionation factors determined in this study if a different choice is made for the reference values of $\delta^{18}O$ and $\delta^{17}O$ of O_2 in atmospheric air with respect to $\delta^{17}O$ and $\delta^{18}O$ of H_2O of VSMOW.

2.2.2. O_2 purification and isotopic analysis

The air samples collected in the closed chambers were transported to LSCE for analyses of the isotopic composition of O_2. The flasks were connected on a semi-automatic separation line inspired from Barkan and Luz (2003) which was made up of 8 ports in which 2 standards (outside air) and 6 samples were analyzed daily (Brandon et al., 2020). After pumping the whole line, the air was circulated through a water trap (ethanol at - 100°C) and then through a carbon dioxide trap immersed in liquid nitrogen at – 196 °C. After collection of the gas samples on a molecular sieve trap cooled at – 196 °C, a helium flow carried it through a chromatographic column which was immersed in a water reservoir at 0 °C to separate the dioxygen and the argon from the dinitrogen. After separation of the dioxygen and argon from helium, the gas was collected in a stainless-steel manifold immersed in liquid helium at – 269 °C.

After collection, the samples were analyzed by the IRMS previously mentioned for leaf water analyses. The following ratios were measured: $^{18}O/^{16}O$, $^{17}O/^{16}O$ and O_2/Ar (as an indicator of the O_2 concentration because Ar is an inert gas). $\delta^{17}O$ and $\delta^{18}O$ of O_2 each sample were obtained through 3 series of 24 dual inlet measurements against a standard made of O_2 and Ar. This sequence was followed by 2 peak jumping analyses of the O_2/Ar ratio including separate measurements of the O_2 and Ar signals for both the standard and the sample. The uncertainty associated with each measurement was obtained from the standard deviation of the three runs and from the repeated peak jumping measurement for $\delta O_2/Ar$ which was defined by $\left[\frac{\left(\frac{n(O_2)}{n(Ar)}\right)sample}{\left(\frac{n(O_2)}{n(Ar)}\right)standard} - 1\right] * 1000$, and $n(O_2)$ is the number of moles of O_2 and $n(Ar)$ the number of moles of Ar. The uncertainty values for $\Delta^{17}O$, $\delta^{18}O$ and $\delta O_2/Ar$ were respectively 10 ppm, 0.05 ‰ and 0.5 ‰.

Each day, we performed measurements of the dioxygen isotopic composition and O_2/Ar ratio on two samples of outside air which is the standard for the isotopic composition of O_2 (Hillaire-Marcel et al., 2021). So that the calibrated $\delta^{18}O$ value for our sample was calculated as in equation 2:

$$\delta^{18}O_{calibrated} = \left[\frac{(\delta^{18}O_{measured}/1000)+1}{(\delta^{18}O_{outsideair}/1000)+1} - 1\right] \times 1000 \quad (2)$$

2.3. Experimental runs

2.3.1. General strategy

Our goal was to calculate the fractionation factor associated with $\delta^{17}O$ and $\delta^{18}O$ for soil respiration, dark leaf respiration and photosynthesis using the microcosm described above. In order to quantify the fractionation factors, we needed to work in closed and controlled conditions. Given the volume of the closed chamber (120 dm^3, hence about 1.12 moles of O_2) and the order of magnitude of dark respiration (order of magnitude of 0.08 μmol O_2 s^{-1} for soil respiration) and net photosynthetic fluxes (order of magnitude of 0.45 μmol O_2 s^{-1}) inside the chamber, we calculated that experiments should last from 3 days to more than 2 weeks so that more than one tenth of the O_2 in the chamber can be recycled by the plant and soil. This recycling allows the creation of sufficiently large isotopic signals (especially $\Delta^{17}O$ of O_2) to be detected and measured. We set up two different experiments in the closed chamber, each experiment being repeated 3 or 4 times to characterize the experimental repeatability of the system.

The first experiment (repeated 4 times, i.e. in 4 sequences) aimed at studying the fractionation factors during soil respiration. The second experiment (repeated 3 times, i.e. in 3 sequences, each sequence being divided into several periods with or without light) aimed at studying the fractionation factors during dark respiration and photosynthesis of plants.

Prior to the aforementioned experiments, measurements were carried out on a closed empty chamber to check the absence of leaks as well as the absence of isotopic fractionation (Table S2).

2.3.2. Soil respiration experiment

To conduct the soil respiration experiment, 2.6 kg of soil (*Terreau universel, Botanic*) were placed in 12 different pots. The light was turned off during this experimental run (Table S1). We decided not to apply any diurnal cycles during dark respiration experimentations for two reasons. First, we wanted to prevent the development of algae, mosses or any photosynthetic organisms in the chamber. Secondly, it was easier to optimize temperature control as the light radiation could increase the temperature inside the closed chamber. During this dark period, CO_2 from soil respiration accumulates in the biological closed chamber. To have a stable concentration of CO_2 during the whole dark period, the CO_2 was trapped using soda lime. Four sequences were performed with respective durations of 53, 51, 43 and 36 days.

2.3.3. Photosynthesis and dark respiration experiment

We used the same soil with plants (*Festuca arundinacea)* grown before the start of the three sequences of the photosynthesis and dark respiration experiment. In order to obtain a significant change of the $\Delta^{17}O$ of O_2 signal in our closed 120 dm^3 chambers, the 3 experiments were run for 1 to 2 months. CO_2 level was controlled to 400 ppm by a CO_2 trap and CO_2 injections. This was done to ensure that the CO_2 in the chamber did not reach levels too far from the atmospheric composition as this could have affected the physiology of the plant. This could have affected the physiology of the plant. The light cycle was controlled to alternate between day (photosynthesis and respiration) and night conditions (respiration) (Table S1).

The values of the leaf water measurements are presented in supplementary Table S3. Because the experiments had to be carried in a closed chamber, we could not sample leaves during the experiment and only got a value at the end of each sequence. Nevertheless, we could compare the isotopic composition of the irrigation and soil water at the start and at the end of the experiment.

2.4. Quantification of fractionation factors

We detail below how we used the results from our experiments to quantify the associated fractionation factors. Notations used below are gathered in Table 1.

The isotopic fractionation factor of oxygen is expressed through the fractionation factor α.

$$^{18}\alpha = \frac{^{18}R_{product}}{^{18}R_{susbtrat}} \quad (3)$$

where α is the fractionation factor and ^{18}R is the ratio of the concentration $^{18}R = \frac{n(^{18}O)}{n(^{16}O)}$ with n the number of moles of O_2 containing ^{18}O or ^{16}O. ^{18}R is linked to the $\delta^{18}O$ value through:

$$\delta^{18}O = \left(\frac{^{18}R_{sample}}{^{18}R_{standard}} - 1\right) \times 1000 \quad (4)$$

The isotopic discrimination is related to the isotopic fractionation factor through:

$$^{18}\varepsilon = {}^{18}\alpha - 1 \quad (5)$$

The same equations (3), (4) and (5) can be proposed for $\delta^{17}O$ and the relationship between the fractionation factors $^{17}\alpha$ and $^{18}\alpha$ is written as:

$$\theta = \frac{\ln {}^{17}\alpha}{\ln {}^{18}\alpha} \quad (6)$$

In some studies, referred to later, the notation γ is also used with $\gamma = \frac{^{17}\varepsilon}{^{18}\varepsilon}$.

2.4.1. Soil respiration

Respiration is associated with isotopic fractionation. The light isotopes, ^{16}O, are more easily integrated by microorganisms than the heavy isotopes, ^{18}O, which hence remain in the atmosphere. We express the fractionation factor for soil respiration as:

$$^{18}\alpha_{soil\_respi} = \frac{^{18}R_{respired}}{^{18}R_{air}} \quad (7)$$

In our experiment, the respiratory process took place in a closed reservoir so that we could calculate the fractionation factors from the evolution of the concentration and isotopic composition of dioxygen in the chamber. The number of molecules of dioxygen in the air of the closed chamber, $n(O_2)$, between time t and time t+dt can be written as:

$$n(O_2)_{t+dt} = n(O_2)_t - dn(O_2) \quad (8)$$

with $dn(O_2)$ the number of dioxygen molecules respired during the time period dt. A similar equation can be written for the number of dioxygen molecules containing ^{18}O remaining in the air of the chamber:

$$^{18}R_{t+dt} \times n(O_2)_{t+dt} = {}^{18}R_t \times n(O_2)_t - {}^{18}R_t \times {}^{18}\alpha_{soil\_respi} \times dn(O_2) \quad (9)$$

The evolution of the isotopic ratio of oxygen, ^{18}R, between time t and time t+dt can be written as:

$$^{18}R_{t+dt} = {}^{18}R_t + d^{18}R \quad (10)$$

Combining equations Eq. (8), (9) and (10), neglecting the second order term $d^{18}R_t \times dn(O_2)_t$ and integrating from t_0 (starting time of the experiment when the chamber is closed) to t leads to:

$$^{18}\varepsilon_{soil\_respi} = {}^{18}\alpha_{soil\_respi} - 1 = \frac{ln\left(\frac{\frac{\delta^{18}O_t}{1000}+1}{\frac{\delta^{18}O_{t0}}{1000}+1}\right)}{\ln\left(\frac{n(O_2)_t}{n(O_2)_{t0}}\right)} \quad (11)$$

Because argon is an inert gas, we can link $\frac{n(O_2)_t}{n(O_2)_{t0}}$ to $\delta\left(\frac{O_2}{Ar}\right)$, so that:

$$\frac{n(O_2)_t}{n(O_2)_{t0}} = \frac{\frac{\delta\left(\frac{O_2}{Ar}\right)_t}{1000}+1}{\frac{\delta\left(\frac{O_2}{Ar}\right)_{t0}}{1000}+1} \quad (12)$$

2.4.2. Dark respiration

In order to calculate the isotopic fractionation associated with soil and plant respiration during dark period, we followed the same calculation as for the soil respiration (section 2.4.1). In this case, we selected only night periods from each sequence of the photosynthesis and dark respiration experiment.

2.4.3. Photosynthesis

During photosynthesis, the oxygen atoms in the dioxygen produced by the plant comes from the oxygen atom of water consumed by photosynthesis in the leaves so that the fractionation factor during photosynthesis can be expressed as:

$$^{18}\alpha_{photosynthesis} = \frac{^{18}R_{produced\ O_2}}{^{18}R_{lw}} \quad (13)$$

where *lw* stands for leaf water.
For our study of *Festuca arundinacea* we consider that the water in the mesophyll layer can be represented by bulk leaf water.

Photosynthesis occurs during the light periods. However, it should be noted that dark respiration, photorespiration and Mehler reaction occur at the same time. In a first approach, we did the assumption that respiration rates remain the same during the light and dark periods. This assumption is probably true for soil respiration since flux of heterotrophic dark respiration is not expected to change for different light conditions if the other environmental drivers (e.g. humidity, temperature, soil organic matter) are constant. However, autotrophic dark respiration is expected to decrease during light periods compared to dark periods. As a consequence, we present sensitivity tests to the dependence of a vanishing dark respiration of leaves during the dark period in Table S4.

Thus, at each stage, dioxygen is both produced by photosynthesis and consumed by the aforementioned O_2 uptake processes (hereafter $total\_respi$) by the plant according to the mass conservation equation:

$$n(O_2)_{t+dt} = n(O_2)_t - dn_{total\_respi} + dn_{photosynthesis} \quad (14)$$

where dn_{total_respi} is the number of molecules of O_2 consumed by dark respiration, photorespiration and Mehler reaction between time t and t+dt, and $dn_{photosynthesis}$ is the number of molecules of O_2 produced by photosynthesis between t and t+dt.

The budget for ^{18}O of O_2 can be written as:

$$^{18}R_{t+dt} \times \frac{n(O_2)_{t+dt}}{n(O_2)_{t0}} = {}^{18}R_t \times \frac{n(O_2)_t}{n(O_2)_{t0}} - {}^{18}R_t \times {}^{18}\alpha_{total\_respi} \times \frac{dn_{total\_respi}}{n(O_2)_{t0}} + {}^{18}R_{lw} \times {}^{18}\alpha_{photosynthesis} \times \frac{dn_{photosynthesis}}{n(O_2)_{t0}} \quad (15)$$

where $^{18}\alpha_{total\_respi}$ is the fractionation factors associated with each O_2 consuming process periods throughout the whole experiment.

We introduced the normalized fluxes of photosynthesis and total respiration as:

$$F_{photosynthesis} = \frac{dn_{photosynthesis}}{n(O_2)_{t0} \times dt} \quad (16)$$

$$F_{total\_respi} = \frac{dn_{total\_respi}}{n(O_2)_{t0} \times dt} \quad (17)$$

$$a^{18}R = \frac{d^{18}R}{dt} \quad (18)$$

This led to the following expression of $^{18}\alpha_{photosynthesis}$:

$$^{18}\alpha_{photosynthesis} = \frac{n(O_2)_t / n(O_2)_{t0} \times a^{18}R + {}^{18}R_t \times \left(F_{photosynthesis} - F_{total_{respi}} + {}^{18}\alpha_{total_{respi}} \times F_{total_{respi}} \right)}{{}^{18}R_{lw} \times F_{photosynthesis}} \quad (19)$$

This equation can be simplified at t=0 for $^{18}R_t$=$^{18}R_{t0}$=1 and $n(O_2)_t$= $n(O_2)_{t0}$:

$^{18}\alpha_{photosynthesis}$ depends on the values of $^{18}\alpha_{total\_respi}$ and of F_{total_respi}, themselves dependent on the values of $^{18}\alpha_{Mehler}$ (fractionation factor associated with Mehler reaction), F_{Mehler} (flux of oxygen related to Mehler reaction), $^{18}\alpha_{dark\_respi}$, F_{dark_respi}, $^{18}\alpha_{photorespi}$ (fractionation factor associated with photorespiration) and $F_{photorespi}$ (photorespiration flux of oxygen). These last 4

parameters could not be determined in our global experiment. Our determination of ${}^{18}\alpha_{photosynthesis}$ will thus rely on assumptions for the estimations of ${}^{18}\alpha_{Mehler}$, F_{Mehler}, ${}^{18}\alpha_{photorespi}$ and $F_{photorespi}$.

To separate the ${}^{18}\alpha_{dark\_respi}$ from the other fractionation factors, we defined:

$$ {}^{18}\alpha_{total\_respi} = {}^{18}\alpha_{photorespi} \times f_{photorespi} + {}^{18}\alpha_{Mehler} \times f_{Mehler} + {}^{18}\alpha_{dark\_respi} \times f_{dark\_respi} \quad (20)$$

with

$$ F_{total\_respi} = F_{dark\_respi} + F_{photorespi} + F_{Mehler} \quad (21)$$

f indicates the fraction of the total oxygen uptake flux corresponding to each process (dark respiration, photorespiration and Mehler reaction) so that:

$$ f_{dark\_respi} + f_{photorespi} + f_{Mehler} = 1 \quad (22)$$

$$ F_{dark\_respi} = f_{dark\_respi} \times F_{total\_respi} \quad (23)$$

$$ F_{photorespi} = f_{photorespi} \times F_{total\_respi} \quad (24)$$

$$ F_{Mehler} = f_{Mehler} \times F_{total\_respi} \quad (25)$$

In the absence of further constraints, we used here as first approximation the global values from Landais et al. (2007) for f_{dark_respi} (0.6), $f_{photorespi}$ (0.3) and f_{Mehler} (0.1). Values for $\alpha_{photorespi}$ and α_{Mehler} were based on the most recent estimates of Helman et al. (2005).

Table 1. List of variables used to quantify fractionations and their definitions. * means either oxygen 17 or oxygen 18.

Symbol	Definition	Origin of the value
${}^{*}\alpha$	Fractionation factor	

${}^{*}\alpha_{dark\_respi}$	Fractionation factor of soil and plant respiration during night periods	Determined by our study
${}^{*}\alpha_{dark\_leaf\_respi}$	Fractionation factor of leaf respiration during night periods	Determined by our study
${}^{*}\alpha_{Mehler}$	Fractionation factor associated with Mehler respiration	Value from Helman et al. (2005)
${}^{*}\alpha_{photorespi}$	Fractionation factor associated with photorespiration	Value from Helman et al. (2005)
${}^{*}\alpha_{photosynthesis}$	Fractionation factor associated with photosynthesis	Determined by our study
${}^{*}\alpha_{soil\_respi}$	Fractionation factor associated with soil respiration	Determined by our study
${}^{*}\alpha_{total\_respi}$	Fractionation factor associated with total respiration during light period	Determined by our study
${}^{*}\varepsilon$	Isotopic discrimination	
${}^{*}\varepsilon_{dark\_respi}$	Isotopic discrimination of soil and plant respiration during night periods	Determined by our study
${}^{*}\varepsilon_{dark\_leaf\_respi}$	Isotopic discrimination of leaf respiration during night periods	Determined by our study
${}^{*}\varepsilon_{photosynthesis}$	Isotopic discrimination associated with photosynthesis	Determined by our study
${}^{*}\varepsilon_{soil\_respi}$	Isotopic discrimination of soil respiration associated with soil respiration experiment	Determined by our study
θ	Ratio of $ln({}^{17}\alpha)\ to\ ln({}^{18}\alpha)$	
θ_{dark_respi}	Ratio of $ln({}^{17}\alpha_{dark\_respi})\ to\ ln({}^{18}\alpha_{dark\_respi})$	Determined by our study
$\theta_{dark\_leaf\_respi}$	Ratio of $ln({}^{17}\alpha_{dark\_leaf\_respi})\ to\ ln({}^{18}\alpha_{dark\_leaf\_respi})$	Determined by our study
$\theta_{photosynthesis}$	Ratio of $ln({}^{17}\alpha_{photosynthesis})\ to\ ln({}^{18}\alpha_{photosynthesis})$	Determined by our study
θ_{soil_respi}	Ratio of $ln({}^{17}\alpha_{soil\_respi})\ to\ ln({}^{18}\alpha_{soil\_respi})$	Determined by our study

aN	Linear regression coefficient of the evolution of $n(O_2)$ as a function of time	Determined by our study
a^*R	Linear regression coefficient of the evolution of R^*O as a function of time	Determined by our study
$dn_{photosynthesis}$	Number of moles of O_2 produced by photosynthesis between t and t+dt	Determined by our study
dn_{total_respi}	Number of moles of O_2 consumed by total respiration during light periods between time t and t+dt	Determined by our study
F_{dark_respi}	Dark respiration flux (normalized vs number of moles of O_2 at the start of the experiment)	Determined by our study
F_{Mehler}	Mehler flux (normalized vs number of moles of O_2 at the start of the experiment)	Determined by our study and Landais et al. (2007)
$F_{photorespi}$	Photorespiration O_2 flux (normalized vs number of moles of O_2 at the start of the experiment)	Determined by our study and Landais et al. (2007)
$F_{photosynthesis}$	Photosynthesis O_2 flux (normalized vs number of moles of O_2 at the start of the experiment)	Determined by our study
F_{total_respi}	Total respiration O_2 flux during light period (normalized vs number of moles of O_2 at the start of the experiment)	Determined by our study
f_{dark_respi}	Fraction of the dioxygen flux corresponding to dark respiration process	Value from Landais et al. (2007)
f_{Mehler}	Fraction of the dioxygen flux corresponding to Mehler process	Value from Landais et al. (2007)
$f_{photorespi}$	Fraction of the dioxygen flux corresponding to photorespiration process	Value from Landais et al. (2007)
$n(O_2)$	Number of moles of O_2	Determined by our study
${}^*R$	Ratio of heavy (^{18}O or ^{17}O) isotope to light isotope (^{16}O) of O_2 in air	Determined by our study
${}^*R_{lw}$	${}^*R$ of leaf water	Determined by our study

3.Results

3.1. Soil Respiration

3.1.1. Experimental data

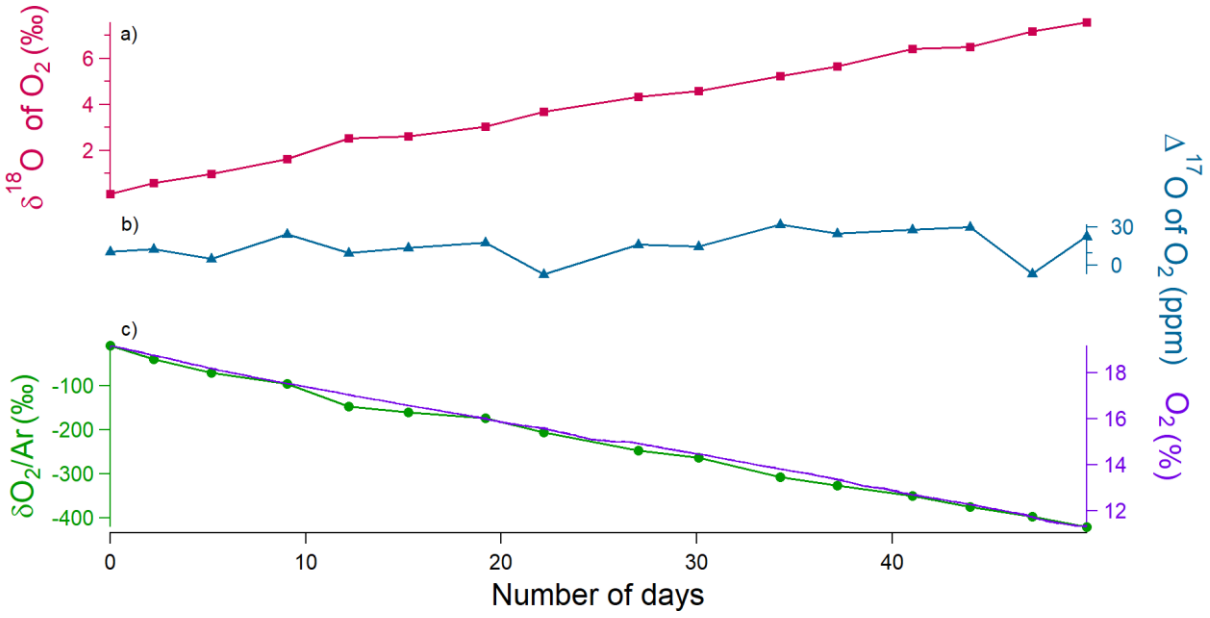

Fig.2. Evolution of the different concentrations and isotopic ratios in the sequence 2 of the soil respiration experiment (day 0 is the beginning of the sequence). (a) $\delta^{18}O$ of O_2 (red) variations. (b) $\Delta^{17}O$ of O_2 (blue) variations. (c) Dioxygen concentration (purple) from the optical sensor and $\delta O_2/Ar$ variations (green) measured by IRMS.

During the 4 sequences, the respiration activity led to a decreasing level of the O_2 concentration measured by the optical sensor or through the $\delta O_2/Ar$ evolution from IRMS measurements (Fig. S1). The comparison of the evolution of the O_2 concentration during the different sequences showed that respiratory fluxes were different with a maximum factor of 4 between the different sequences (Fig. S1). In parallel to the decrease in O_2 concentration, the $\delta^{18}O$ increased as expected because respiration preferentially consumes the lightest isotopes: over the 51 days of the 2nd soil respiration sequence, we observed a linear decrease of oxygen concentration by more than 5 % while $\delta^{18}O$ increased by 8 ‰ (Fig. 2). A Mann-Kendall trend test showed that the $\Delta^{17}O$ of O_2 does not show any statistically significant trend over the 4 sequences (Fig. S2) (p-values were equal to 0.40, 0.08, 0.58, 0.47, respectively).

3.1.2. Fractionation factors

We used the 15 to 20 samples obtained during each sequence of soil respiration experiment to draw the relative evolution of $ln({}^{18}R_t/{}^{18}R_{t0})$ vs $ln\left((\delta\left(\frac{O_2}{Ar}\right)_t/1000+1)/(\delta\left(\frac{O_2}{Ar}\right)_{t0}/1000+1)\right)$ following Eq. (11) (Fig. 3). The slope of the corresponding regression line provided the isotopic

discrimination $^{18}\varepsilon_{soil\_respi}$ and hence the fractionation factor $^{18}\alpha_{soil\_respi}$ for each sequence (Table S5). It could be observed that despite differences in respiratory fluxes for the different sequences (the standard deviation is equal to 50 % of the average flux across sequences; see Table S5), the relationship between $\delta^{18}O$ of O_2 and O_2 concentration (or $\delta O_2/Ar$), and hence the calculated fractionation factor associated with respiration, is not much affected.

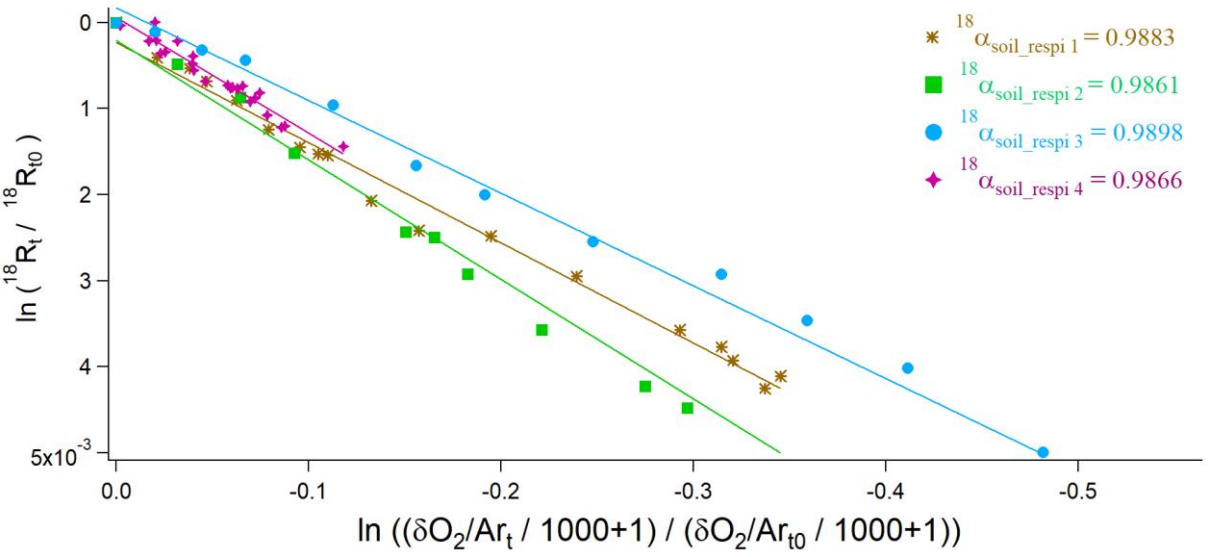

Fig.3 Determination of $^{18}O/^{16}O$ fractionation factors in the 4 respiration sequences. $^{18}\alpha_{soil\_respi\ 1}$ (brown), $^{18}\alpha_{soil\_respi\ 2}$ (green), $^{18}\alpha_{soil\_respi\ 3}$ (blue), $^{18}\alpha_{soil\_respi\ 4}$ (purple) are respectively respiratory fractionation factors associated with sequences 1 to 4.

Using the results of the 4 sequences, we determined the values for the mean isotopic discrimination $^{18}\varepsilon_{soil\_respi}$ (- 12.3 ± 1.7 ‰), the mean isotopic discrimination $^{17}\varepsilon_{soil\_respi}$ (- 6.4 ± 0.9 ‰) and the average θ_{soil_respi} (0.5164 ± 0.0005).

3.2. Photosynthesis and dark respiration

3.2.1. Experimental data

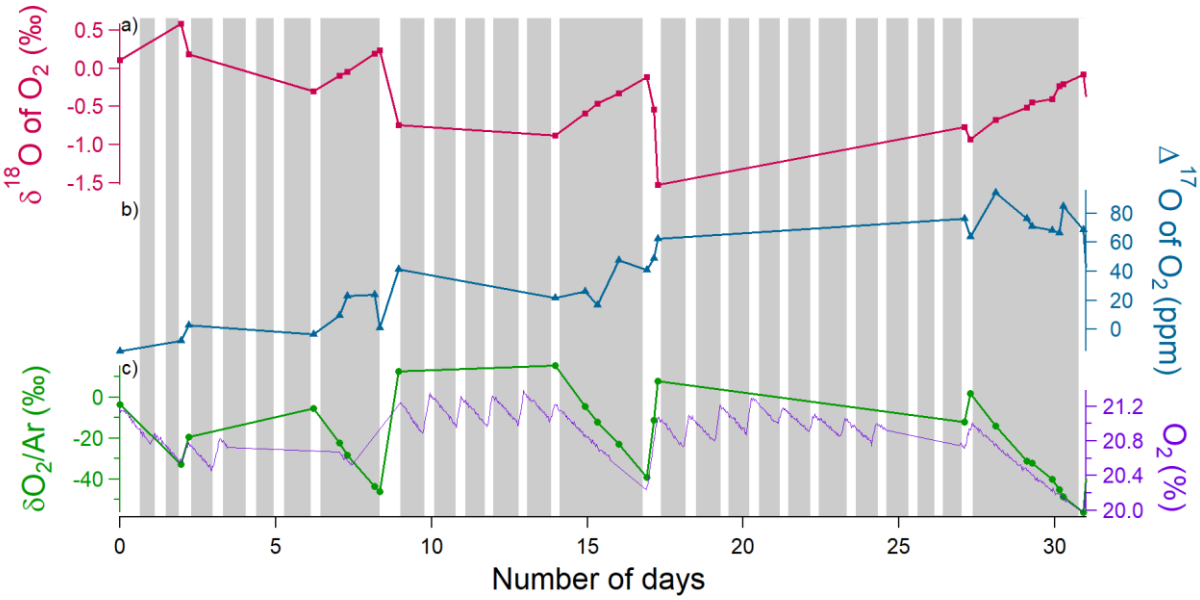

Fig.4. Example of the evolution of the different concentrations and isotopic ratios in the sequence 1 of photosynthesis and dark respiration experiment in the closed chamber over 31 days (day 0 is the beginning of the sequence). Grey rectangles correspond to night periods and white rectangles to light periods. (a) $\delta^{18}O$ of O_2 (red) variations. (b) $\Delta^{17}O$ of O_2 variations (blue). (c) Dioxygen concentration (purple) from the optical sensor and $\delta O_2/Ar$ variations (green) measured by IRMS.

During the night periods, when only respiration occurred, we observed a decrease in O_2 concentration by 1% within 3 days and a $\delta^{18}O$ increase by 1‰ during the same period (Fig. 4). The evolution was qualitatively similar with that of soil respiration experiments with higher fluxes. We observed the same trends for the evolution of $\delta O_2/Ar$ during the night periods as for the respiration experiment. During light periods, there was a marked decrease in $\delta^{18}O$ (2 ‰) and a marked increase in the flux of oxygen released (1%) during 1 day. We observed the same trends for the evolution of $\delta O_2/Ar$ during the night periods as for the respiration experiment.

The Mann-Kendall test (95%) showed a significative increasing trend of the $\Delta^{17}O$ of O_2 over sequences 1 and 2 (Fig. S3) ($\simeq$ 100 ppm in 31 days for sequence 1, $\simeq$ 100 ppm in 40 days for sequence 2) while no significant increase of $\Delta^{17}O$ of O_2 is observed over sequence 3 (Fig. S3).

3.2.2. Fractionation factors

Dark respiration

The average of the isotopic discrimination for dark respiration ${}^{18}\varepsilon_{dark\_respi}$ and ${}^{17}\varepsilon_{dark\_respi}$ were calculated over the 9 night periods and we obtained values of respectively - 17.0 ± 2.0 ‰ and - 8.5 ±

0.8 ‰. The average of θ_{dark_respi} during the experiment was equal to 0.5124 ± 0.0084 (details in Table S6).

The dark respiration of this experiment includes respiration of both soil and leaves. Because soil respiration fractionation factor has been determined above, it is possible to estimate here the fractionation factor for the dark leaf respiration and we consider that respiration rate during dark and light periods do not vary:

$$F_{dark\_respi} = F_{soil\_respi} + F_{dark\_leaf\_respi} \quad (26)$$

$$^{18}\alpha_{dark\_respi} = f_{soil\_respi} \times {}^{18}\alpha_{soil\_respi} + f_{dark\_leaf\_respi} \times {}^{18}\alpha_{dark\_leaf\_respi} \quad (27)$$

with $F_{dark\_leaf\_respi}$ the flux of leaf respiration during the night, f_{soil_respi} the fraction of soil respiration during night periods (F_{soil_respi} / F_{dark_respi}) and $f_{dark\_leaf\_respi}$ the fraction of dark leaf respiration during night periods ($F_{dark\_leaf\_respi}$ / F_{dark_respi}).

$$^{18}\alpha_{dark\_leaf\_respi} = \frac{^{18}\alpha_{dark\_respi} - f_{soil\_respi} \times {}^{18}\alpha_{soil\_respi}}{f_{dark\_leaf\_respi}} \quad (28)$$

The isotopic discriminations $^{18}\varepsilon_{dark\_leaf\_respi}$ and $^{17}\varepsilon_{dark\_leaf\_respi}$ were respectively equals to -19.1 ± 2.4 ‰ and - 9.7 ± 0.9 ‰. The average of $\theta_{dark\_leaf\_respi}$ was equal to 0.5089 ± 0.0777. The standard deviations (1σ) was calculated by a Monte Carlo method from the individual uncertainties of the $^{18}\alpha_{dark\_respi}$, $^{18}\alpha_{soil\_respi}$, F_{soil_respi} and F_{dark_respi}.

Photosynthesis

In order to calculate an average value for the fractionation factor associated with photosynthesis from Eq. (19), we first calculated the averages of the flux of the O_2 consuming processes and of the fractionation factors associated with each sequence: $\langle F_{total\_respi} \rangle$ and $\langle {}^{18}\alpha_{total\_respi} \rangle$. We also calculated the net O_2 flux during light periods, $aN = F_{photosynthesis} - F_{total\_respi}$, as the linear regression, aN, of $\frac{n(O_2)_t}{n(O_2)_{t0}}$ with time. $a^{18}R$ is also obtained as a linear regression of ^{18}R with time over

each light period. Our data support our assumption that the regime was stationary over time and $n(O_2)_t / n(O_2)_{t0}$ evolved linearly over time, which is why we were able to do linear regressions.

$$^{18}\alpha_{photosynthesis} = \frac{a^{18}R + aN + \langle ^{18}\alpha_{total\_respi}\rangle \times \langle F_{total\_respi}\rangle}{^{18}R_{lw} \times F_{photosynthesis}} \quad (29)$$

The results of the 8 individuals $\alpha_{photosynthesis}$ values are given in Table S10. The value of isotopic fractionation associated with the light period of period 1 of sequence 1 appeared clearly out of range. Following the Dixon's outlier detection test (Dixon, 1960), this value was considered an anomaly (likelihood > 99 %) and was removed from further analysis.

We finally estimated the values of $^{18}\varepsilon_{photosynthesis}$ and $^{17}\varepsilon_{photosynthesis}$ as + 3.7 ± 1.3 ‰ and + 1.9 ± 0.6 ‰, respectively. The average of $\theta_{photosynthesis}$ was equal to 0.5207 ± 0.0537, a value which depends on the value taken for the $\delta^{17}O$ value of atmospheric O_2 vs VSMOW (Sharp and Wostbrock, 2021), see Table 2.

We performed different sensitivity tests (supplementary texts 1 and 2). Sensitivity test 1 (Table S4) quantifies the influence of vanishing flux of dark leaf respiration during the day. This test shows that the assumption of similar flux of dark leaf respiration during the night and light periods did not influence much the values of photosynthesis fractionation factors. It results in an additional uncertainty of 0.0006 and 0.0005 for the values of $^{18}\alpha_{photosynthesis}$ and $^{17}\alpha_{photosynthesis}$.

Sensitivity tests 2 (Tables S7, S8 and S9) were performed on values of the O_2 flux and associated fractionation factors for photorespiration and Mehler reaction. They resulted in additional uncertainties of 0.0007 and 0.0005 for the values of $^{18}\alpha_{photosynthesis}$ and $^{17}\alpha_{photosynthesis}$ (Table S10).

Sensitivity tests 3 concerned the possible evolution of the isotopic composition of leaf water on the course of an experiment. The comparison of the $\delta^{18}O$ of irrigation water and soil water at the end of the experiment shows a possible increase up to 2‰ (Table S3). We thus estimate that our values of leaf water $\delta^{18}O$ measured at the end of the experiment may be overestimated by 1‰ compared to the mean value of leaf water $\delta^{18}O$ during the course of the experiment. Taking this possible effect into account would lead to a fractionation factor for photosynthesis higher by 1‰ compared to the presented one of 3.7 ± 1.3 ‰, hence a higher isotopic discrimination associated with photosynthesis.

607 Finally, we evaluated by a Monte Carlo calculation how the different uncertainties listed in the 3
608 sensitivity tests described above influence the final uncertainty on the photosynthesis isotopic
609 discrimination. We found a final standard deviations (1σ) equal to 0.3 ‰ for $^{18}\varepsilon_{photosynthesis}$ and
610 0.15 ‰ for $^{17}\varepsilon_{photosynthesis}$.
611

612 # 4.Discussion

613 **4.1. $\Delta^{17}O$ of O_2**

614 The $\Delta^{17}O$ of O_2 is equal to 0 by definition for atmospheric air, and hence it should be equal to zero at
615 the beginning of each experiment. The observed change during an experiment can only be driven by
616 biological processes because the interaction with stratosphere is not possible in the closed chambers.

617 During the soil respiration experimental run, the $\Delta^{17}O$ of O_2 was constant. This directly reflects the
618 θ_{soil_respi} value of 0.5164 ± 0.0005 (Table 2) because $\Delta^{17}O$ of O_2 is defined with a slope of 0.516
619 between $\ln(1+\delta^{17}O)$ and $\ln(1+\delta^{18}O)$ (Eq. 1). This result is in good agreement and within the
620 uncertainties given by Helman et al. (2005) with the γ value of 0.5174(equivalent to a θ of 0.515 ±
621 0.0003) obtained with respiration experiments on several micro-organisms.

622 During the experiment involving both oxygen uptake and photosynthesis, the $\Delta^{17}O$ of O_2 has a globally
623 increasing trend with values reaching about 100 ppm after one month. Such behavior is expected and
624 was already observed by Luz et al. (1999) with $\Delta^{17}O$ of O_2 values reaching 150 ppm after a 200-day
625 experiment within a closed terrarium. This increase cannot be explained by respiration because
626 respiration does not modify $\Delta^{17}O$ of O_2. It can be explained by photosynthesis producing oxygen with
627 a $\Delta^{17}O$ of O_2 different from the atmospheric one. Previous analyses have shown that the $\Delta^{17}O$ of H_2O
628 of VSMOW (close to mean oceanic water) expressed vs isotopic composition of atmospheric O_2 has a
629 value between 134 to 223 ppm (using a definition of $\Delta^{17}O$ of H_2O = $\ln(1+\delta^{17}O)-0.516 \times \ln(1+\delta^{18}O)$)
630 (Sharp and Wostbrock, 2021). Within the water cycle, the slopes of $\ln(1+\delta^{17}O)$ vs $\ln(1+\delta^{18}O)$ for the
631 meteoric line, evaporation and evapotranspiration lines are larger than 0.516 (Li and Meijer, 1998;
632 Landais et al., 2006) so that $\Delta^{17}O$ of water consumed by the plants during photosynthesis should be
633 slightly lower than the $\Delta^{17}O$ of VSMOW expressed vs isotopic composition of atmospheric O_2 but still
634 higher than the $\Delta^{17}O$ of atmospheric O_2. Photosynthesis can thus explain the $\Delta^{17}O$ of O_2 increase in the
635 closed chamber.
636

637 **4.2. Fractionation factors associated with $\delta^{18}O$ of O_2 and implications for the Dole effect**

638 **Table 2. Summary of the mean values of the isotopic discriminations and gamma values for** *Festuca*
639 *arundinacea* **of all sequences of (1) the soil respiration experiment and of (2) the respiration and**
640 **photosynthesis experiment and the number of data on which they were calculated.** ** is the value
641 for $\theta_{photosynthesis}$ that depends on the determination of the $\delta^{17}O$ of atmospheric O_2 vs $\delta^{17}O$ of
642 VSMOW. We provide here the two different possible estimates using either 12.03 ‰ (Luz and Barkan,
643 2011) or 12.08 ‰ (Barkan and Luz, 2005): value determined with $\delta^{17}O$= 12.03 ‰ / value determined
644 with $\delta^{17}O$ = 12.08 ‰.

645

Isotopic discriminations and gamma values of *Festuca arundinacea*	Average (‰)	Standard deviation (‰)	Number of data
$^{18}\varepsilon_{soil\_respi}$	-12.3	1.7	4
$^{17}\varepsilon_{soil\_respi}$	-6.4	0.9	4
θ_{soil_respi}	0.5164	0.0005	4
$^{18}\varepsilon_{dark\_respi}$	-17.0	2.0	9
$^{17}\varepsilon_{dark\_respi}$	-8.5	0.8	9
θ_{dark_respi}	0.5124	0.0084	9
$^{18}\varepsilon_{dark\_leaf\_respi}$	-19.1	2.4	9
$^{17}\varepsilon_{dark\_leaf\_respi}$	-9.7	0.9	9
$\theta_{dark\_leaf\_respi}$	0.5089	0.0777	9
$^{18}\varepsilon_{photosynthesis}$	3.7	1.3	8
$^{17}\varepsilon_{photosynthesis}$	1.9	0.6	8
$\theta_{photosynthesis}$	0.5207/0.5051**	0.0537/0.0504**	8

646

647 The isotopic discrimination $^{18}\varepsilon_{soil\_respi}$ = - 12.3 ± 1.7 ‰ for the soil respiration experiments is
648 comparable to the average terrestrial soil respiration isotopic discrimination found by Angert et al.
649 (2001) of - 12 ‰. Still, among the diversity of soils studied by Angert et al. (2001), the soils showing
650 the $^{18}\varepsilon$ values closest to our values are clay soil ($^{18}\varepsilon$ = - 13 ‰) and sandy soil ($^{18}\varepsilon$ = - 11 ‰). Soil
651 respiration isotopic discriminations are less strong than isotopic discrimination due to dark respiration
652 alone (- 18‰, Bender et al., 1994). These lower values for soil respiration isotopic discrimination are
653 due to the roles of root diffusion in the soil (Angert and Luz, 2001). The soils studied by Angert and Luz
654 (2001) are however different from our soil which was enriched in organic matter. Further experiments
655 are then needed to understand the variability in $^{18}\varepsilon$ associated with soil respiration.

The isotopic discrimination for dark leaf respiration, $^{18}\varepsilon_{dark\_leaf\_respi}$ = - 19.1 ± 2.4 ‰ is associated with a large uncertainty and would benefit from additional experiments with a higher sampling and measurement rate. Still, even if it was obtained on different organisms and experimental set-ups, this value is in agreement with the values for isotopic discrimination for dark respiration determined by Helman et al. (2005) on bacteria from the Lake Kinneret ($^{18}\varepsilon$ = -17.1 ‰) and Synechocystis ($^{18}\varepsilon$ = - 19.4 ‰ and - 19.5 ‰) and Guy et al. (1989) on Phaeodactylum tricornutum and on terrestrial plants (-17 to -19 ‰ for COX respiration).

The average $^{18}\varepsilon_{photosynthesis}$ is + 3.7 ± 1.3 ‰ for *Festuca arundinacea* species which goes against the classical assumption that terrestrial photosynthesis does not fractionate (Vinogradov et al., 1959; Guy et al., 1993; Helman et al., 2005; Luz & Barkan, 2005). Vinogradov explains that the low photosynthetic isotopic discrimination that can occur is due to contamination by atmospheric O_2 or by respiration. Guy et al. (1993) corroborate this idea by finding a photosynthetic isotopic discrimination of 0.3 ‰ in cyanobacteria (Anacystis nidulans) and diatoms (Phaeodactylum tricornutum) that they consider negligible. Luz and Barkan (2005) in their study on *Philodendron*, consider that there is no photosynthetic isotopic discrimination. Our value suggests that there is a terrestrial photosynthetic isotopic discrimination and the value found for *Festuca arundinacea* is slightly smaller than the photosynthetic isotopic discrimination in marine environment $^{18}\varepsilon_{photosynthesis}$ = + 6 ‰ found by Eisenstadt et al. (2010). More specifically, Eisenstadt et al. (2010) determined several photosynthetic isotopic discrimination values depending on the phytoplankton studied (*Phaeodactylum tricornutum* = 4.5 ‰, *Nannochloropsis sp.* = 3 ‰, *Emiliania huxleyi* = 5.5 ‰ and *Chlamydomonas reinhardtii* = 7 ‰). One of the conclusions given by Eisenstadt et al. (2010) is that eukaryotic organisms enrich their produced oxygen more in ^{18}O than prokaryotic organisms. Our conclusion based on experiments performed with *Festuca arundinacea* species is in agreement with these conclusions.

Our experiments were performed at the scale of the plants which is different to previous studies performed at the scale of the chloroplast (e.g. Guy et al., 1993) where no evidence of oxygen fractionation has been found. We can thus not exclude that this fractionation attributed here to photosynthesis is due to oxygen consuming processes not taken into account in our approach. Our main goal however is to interpret the global δ^{18}O of atmospheric O_2 using the fractionation observed at the scale of the plants. As a consequence, we believe that if there is a light-dependent oxygen fractionation process that we did not identify in our approach, it will also be present at the global scale. It should thus be taken into account in our future interpretation of the Dole effect. We thus keep our estimate of the photosynthesis ^{18}O discrimination described above but name it as an *effective* photosynthesis ^{18}O discrimination at the scale of the plants because the details of the processes at play is not fully elucidated.

Finally, we should however note that we tested only one species. Additional experiments with different plants are needed to check if the positive effective fractionation factor should be applied for global Dole effect calculation. Still, this positive *effective* ^{18}O discriminations during photosynthesis suggests that the terrestrial Dole effect may be higher than currently assumed and challenge the assumption that terrestrial and oceanic Dole effects have the same values (Luz and Barkan, 2011).

4-Conclusion

Using a simplified analog of the terrestrial biosphere in a closed chamber we found that the fractionation factors of soil respiration and dark leaf respiration at the biological chamber level agree with the previous estimates derived from studies at micro-organism level. This is an important confirmatory step for the fractionation factors previously used to estimate the global Dole effect. More importantly, we document for the first time a significant *effective* ^{18}O discrimination at the scale of the plant during terrestrial photosynthesis with the *Festuca arundinacea* species (+ 3.7 ‰ ± 1.3 ‰). If confirmed by future studies, this can have a substantial impact on the calculation of the Dole effect, with important consequences for our estimates of the past global primary production.

Our study showed the usefulness of closed chamber systems to quantify the fractionation factors associated with biological processes in the oxygen cycle at the plant level. The main limitation of our present study was the low sampling rate during our experiments which hamper the precision of the determined fractionation factors. Future work should use this validated set-up to multiply such experiments to improve the precision of fractionation factors and to explore the variability of fractionation factors for different plants and hence different metabolisms. A good application would be to study the difference between C3 and C4 plants because C4 plants do not photorespire. C4 plants, adapted to dry environments, have their own strategy and make very little photorespiration through specialized cells. This allows them to produce their own energy in an optimal way without the waste produced by photorespiration.

Data availability

All individual fractionation factors for each experiment are given in the Supplement.

Author contributions

AL and CPi designed the project. CPi, JS and SD carried out experiments at ECOTRON of Montpellier and FP, CPa, RJ, AD and OJ at LSCE. CPa, NP and AL analyzed the data. CPa and AL prepared the manuscript with contributions from NP, CPi, JS and AM.

Competing interests

The authors declare that they have no conflict of interest.

Acknowledgements

The research leading to these results has received funding from the European Research Council under the European Union H2020 Programme (H2020/20192024)/ERC grant agreement no. 817493 (ERC ICORDA) and ANR HUMI17. The authors acknowledge the scientific and technical support of PANOPLY (Plateforme ANalytique géOsciences Paris-sacLaY), Paris-Saclay University, France. This study benefited from the CNRS resources allocated to the French ECOTRONS Research Infrastructure, from the Occitanie Region and FEDER investments as well as from the state allocation 'Investissement d'Avenir' AnaEE- France ANR-11-INBS-0001. We would also like to thank Abdelaziz Faez and Olivier Ravel from ECOTRON of Montpellier for their help, Anne Alexandre from CEREGE at Aix-en-Provence and Emeritus Prof. Phil Ineson from University of York.

References

Alexandre, A., Landais, A., Vallet-Coulomb, C., Piel, C., Devidal, S., Pauchet, S., Sonzogni, C., Couapel, M., Pasturel, M., Cornuault, P., Xin, J., Mazur, J-C., Prié, F., Bentaleb, I., Webb, E., Chalié, F., and Roy, J.: The triple oxygen isotope composition of phytoliths as a proxy of continental atmospheric humidity: insights from climate chamber and climate transect calibrations, Biogeosciences, 15, 3223-3241, https://doi.org/10.5194/bg-15-3223-2018, 2018.

Angert, A., Luz, B., and Yakir, D.: Fractionation of oxygen isotopes by respiration and diffusion in soils and its implications for the isotopic composition of atmospheric O_2, Global Biogeochem. Cy., 15, 871-880, https://doi.org/10.1029/2000GB001371, 2001.

Angert, A., Barkan, E., Barnett, B., Brugnoli, E., Davidson, E. A., Fessenden, J., Maneepong, S.,

Panapitukkul,N., Randerson, J. T., Savage, K., Yakir, D., and Luz, B.: Contribution of soil respiration in tropical, temperate, and boreal forests to the ^{18}O enrichment of atmospheric O_2, Global Biogeochem. Cy., 17, 1089, https://doi.org/10.1029/2003GB002056, 2003.

Barkan, E., and Luz, B.: High precision measurements of $^{17}O/^{16}O$ and $^{18}O/^{16}O$ of O2 and O2/Ar ratio in air, Rapid Commun. Mass Spectrom., 17, 2809-2814, https://doi.org/10.1002/rcm.1267, 2003.

Barkan, E., and Luz, B.: High precision measurements of $^{17}O/^{16}O$ and $^{18}O/^{16}O$ ratios in H_2O, Rapid Commun. Mass Spectrom., 19, 3737-3742, https://doi.org/10.1002/rcm.2250, 2005.

Bauwe, H., Hagemann, M., and Fernie, A.R.: Photorespiration: players, partners and origin, Trends Plant Sci., 6, 330-336, https://doi.org/10.1016/j.tplants.2010.03.006 , 2010.

Bender, M., Sowers, T., Dickson, M-L., Orchardo, J., Grootes, P., Mayewski, P. A., and Meese, D. A.: Climate correlations between Greenland and Antarctica during the past 100,000 years, Nature, 372, 663-666, https://doi.org/10.1038/372663a0, 1994.

Blunier, T., Barnett, B., Bender, M. L., and Hendricks, M. B.: Biological oxygen productivity during the last 60,000 years from triple oxygen isotope measurements, Global Biogeochem. Cy., 16, 3-4, https://doi.org/10.1029/2001GB001460, 2002.

Brandon, M., Landais, A., Duchamp-Alphonse, S., Favre, V., Schmitz, L., Abrial, H., Prié, F., Extier, T., and Blunier, T.: Exceptionally high biosphere productivity at the beginning of Marine Isotopic Stage 11, Nat. Commun., 11, 1-10, https://doi.org/10.1038/s41467-020-15739-2, 2020.

Dansgaard, W.: Stable isotopes in precipitation, Tellus, 16, 436-468, 1974.

Davidson, E.A., Janssens, I.A., and Luo, Y.: On the variability of respiration in terrestrial ecosystems: moving beyond Q10, Glob. Change Biol., 12, 154-164, https://doi.org/10.1111/j.1365-2486.2005.01065.x, 2005.

Dixon, W. J.: Simplified estimation from censored normal sample, Ann. Math. Stat., 21, 488-506, https://doi.org/10.1214%2Faoms%2F1177729747, 1960.

Dole, M.: The Relative Atomic Weight of Oxygen in Water and in Air A Discussion of the Atmospheric Distribution of the Oxygen Isotopes and of the Chemical Standard of Atomic Weights, J. Chem. Phys. 4, 268, https://doi.org/10.1063/1.1749834, 1936.

Dongman, G., Nürnberg, H. W., Förstel, H., and Wagener, K.: On the enrichment of $H_2{}^{18}O$ in the leaves of transpiring plants, Radiat Environ Biophys, 11, 41-52, https://doi.org/10.1007/BF01323099, 1974.

Dreyfus, G. B., Parrenin, F., Lemieux-Dudon, B., Durand, G., Masson-Delmotte, V., Jouzel, J., Barnola[3], J-M., Panno[5], L., Spahni, R., Tisserand, A., Siegenthaler, U., and Leuenberger, M.: Anomalous flow below 2700 m in the EPICA Dome C ice core detected using $\delta^{18}O$ of atmospheric oxygen measurements, Clim. Past, 3, 341-353, https://doi.org/10.5194/cp-3-341-2007, 2007.

Eisenstadt, D., Barkan, E., Luz, B., and Kaplan, A.: Enrichment of oxygen heavy isotopes during photosynthesis in phytoplankton, Photosynth. Res., 103, 97-103, https://doi.org/10.1007/s11120-009-9518-z, 2010.

Extier, T., Landais, A., Bréant, C., Prié, F., Bazin, L., Dreyfus, G., Roche, D. M., and Leuenberger, M.: On the use of $\delta^{18}O_{atm}$ for ice core dating, Quat. Sci. Rev., 185, 244-257, https://doi.org/10.1016/j.quascirev.2018.02.008, 2018.

Guy, R. D., Fogel, M.L., and Berry, J. A.: Photosynthetic fractionation of the stable isotopes of oxygen and carbon, Plant Physiol., 101, 37-47, https://doi.org/10.1104/pp.101.1.37, 1993.

Helman, Y., Barkan, E., Eisenstadt, D., Luz, B., and Kaplan, A.: Fractionation of the three stables oxygen isotopes by oxygen-producing and oxygen-consuming reactions in photosynthetic organisms, Plant Physiol., 138, 2292-2298, https://doi.org/10.1104/pp.105.063768, 2005.

Hillaire-Marcel, C., Kim, S-T., Landais, A., Ghosh, P., Assonov., S., Lécuyer, C., Blanchard, M., Meijer, H. A. J., and Steen-Larsen, H.: A stable isotope toolbox for water and inorganic carbon cycle studies, Nat. Rev. Earth Environ, 2, 699-719, https://doi.org/10.1038/s43017-021-00209-0 , 2021.

Hoffmann, G., Cuntz, M., Weber, C., Ciais, P., Friedlingstein, P., Heimann, M., Jouzel, J., Kaduk, J.,

817 Maier Reimer, E., Seibt, U., and Six, K.: A model of the Earth's Dole effect, Global Biogeochem. Cy.,
818 18, 1-15, https://doi.org/10.1029/2003GB002059, 2004.

819 Keenan, T.F., Migliavacca M., Papale, D., Baldocchi, D., Reichstein, M., Torn, M., and Wutzler, T.:
820 Widespread inhibition of daytime ecosystem respiration, Nat. Ecol. Evol., 3, 407-415,
821 https://doi.org/10.1038/s41559-019-0809-2, 20194.

822

823 Landais, A., Barkan, E., Yakir, D., and Luz, B.: The triple isotopic composition of oxygen in leaf water,
824 Geochim. Cosmochim. Ac., 70, 4105-4115, https://doi.org/10.1016/j.gca.2006.06.1545, 2006.
825

826 Landais, A., Dreyfus, G., Capron, E., Masson-Delmotte, V., Sanchez-Goñi, M. F., Desprat, S.,
827 Hoffmann, G., Jouzel, J., Leuenberger and M., Johnsen, S.: What drives the orbital and millennial
828 variations of $d^{18}O_{atm}$?, Quat. Sci. Rev., 29, 235-246, https://doi.org/10.1016/j.quascirev.2009.07.005,
829 2010.
830

831 Luz, B., and Barkan, E.: The isotopic composition of atmospheric oxygen, Global Biogeochem. Cy.,
832 25, GB3001, https://doi.org/10.1029/2010GB003883, 2011.
833

834 Luz, B., Barkan, E., Bender, M. L., Thiemens, M. H., and Boering, K. A.: Triple-isotope composition of
835 atmospheric oxygen as a tracer of biosphere productivity, Nature, 400, 547-550,
836 https://doi.org/10.1038/22987, 1999.
837

838 Malaizé, B., Paillard, D., Jouzel, J., and Raynaud, D.: The Dole effect over the Last two glacial-
839 interglacial cycles, J. Geophys. Res., 104, 14199-14208, https://doi.org/10.1029/1999JD900116,
840 1999.
841 Mehler, A.: Studies on reactions of illuminated chloroplasts: I. Mechanism of the reduction of
842 oxygen and other hill reagents, Arch. Biochem. Biophys., 33, 65–77,
843 https://doi.org/10.1016/00039861(51)90082-3, 1951.
844

845 Meijer, H. A. J., and Li, W. J.: The use of electrolysis for accurate $\delta^{17}O$ and $\delta^{18}O$ Isotope
846 Measurements in Water, Isot. Environ. Health Stud., 34, 349-369,
847 https://doi.org/10.1080/10256019808234072, 1998.
848

849 Milcu, A., Allan, E., Roscher, C., Jenkins, T., Meyer, S. T., Flynn, D., Bessler, H., Buscot, F.,

Engels, C., Gubsch, M., König, S., Lipowsky, A., Loranger, J., Renker, C., Scherber, C., Schmid, B., Thébault, E., Wubet, T., Weisser, W. W., Scheu, S., and Eisenhauer, N.: Functionally and phylogenetically diverse plant communities key to soil biota, Ecology, 94, 1878-1885, https://doi.org/10.1890/12-1936.1, 2013.

Pack, A., Höweling, A., C.Hezel, D., T.Stefanak, M., Beck, A-K., T. M.Peters, S., Sengupta, S., Herwartz, D., and Folco, L.: Tracing the oxygen isotope composition of the upper Earth's atmosphere using cosmic spherules, Nat. Commun, 8, 1502, https://doi.org/10.1038/ncomms15702, 2017.

Reutenauer, C., A. Landais, A., T. Blunier, T., C. Bréant, C., M. Kageyama, M., M.-N. Woillez, M-N., Risi, C., Mariotti, V., and P. Braconnot, Quantifying molecular oxygen isotope variations during a Heinrich stadial, Clim. Past, 11, 1527-1551, https://doi.org/10.5194/cp-11-1527-2015, 2015.

Ribas-Carbo, M., Berry, J.A., Yakir, D., Giles, L., Robinson, S.A., Lennon, A.M., andSiedow, J.N.: Electron Partitioning between the Cytochrome and Alternative Pathways in Plant Mitochondria, Plant Physiol., 109, 829-837, https://doi.org/10.1104/pp.109.3.829, 1995.

Seltzer, A. M., Severinghaus, J. P., Andraski, B. J., and Stonestrom, D. A.: Steady state fractionation of heavy noble gas isotopes in a deep unsaturated zone, Water Resour. Res., 53, 2716-2732, https://doi.org/10.1002/2016WR019655, 2017.

Severinghaus, J. P., Beaudette, R., Headly, M. A., Taylor, K. and Brook, E. J.: Oxygen-18 of O_2 records the impact of abrupt climate change on the terrestrial biosphere, Science, 324, 1431-1434, https://doi.org/10.1126/science.1169473, 2009.

Shackleton, N. J.: The 100,000-Year Ice-Age Cycle Identified and Found to Lag Temperature, Carbon Dioxide, and Orbital Eccentricity, Science, 289, 1897-1902, https://doi.org/10.1126/science.289.5486.1897, 2000.

Sharkey, T.D., Badger, M.R., von Caemmerer, S., and Andrews, T.J.: High Temperature Inhibition of Photosynthesis Requires Rubisco Activase for Reversibility, Trends Plant Sci., 2465-2468, https://doi.org/10.1007/978-94-011-3953-3_577, 1998.

Sharp, Z. D., and Wostbrock, J. A. G.: Standardization for the Triple Oxygen Isotope System: Waters, Silicates, Carbonates, Air, and Sulfates, Rev. Mineral. Geochem., 86, 179-196, https://doi.org/10.2138/rmg.2021.86.05, 2021.

Stolper, D. A., Fischer, W. W., and Bender, M. L.: Effects of temperature and carbon source on the isotopic fractionations associated with O_2 respiration for $^{17}O/^{16}O$ and $^{18}O/^{16}O$ ratios in *E. coli*, Geochim. Cosmochim. Ac., 240, 152-172, https://doi.org/10.1016/j.gca.2018.07.039, 2018.

Tcherkez, G., and Farquhar, G.D.: On the $^{16}O/^{18}O$ isotope effect associated with photosynthetic O_2 production, Funct. Plant Biol., 34, 1049-1052, https://doi.org/10.1071/FP07168, 2007.

Tcherkez, G., Gauthier, P., Buckley, T.N, Bush, F.A., Barbour, M.M., Bruhn, D., Heskel, M.A., Gong, X.Y., Crous, K.Y., Griifin, K., Way, D., Turnbull, M., Adams, M.A., Atkin, O.K., Farquhar, G.D., and Cornic, G.: Leaf day respiration: low CO2 flux but high significance for metabolism and carbon balance, New Phytol., 216, 986-1001, https://doi.org/10.1111/nph.14816, 2017.

Vinogradov, A. P., Kutyurin, V.M., and Zadorozhnyi, I.K.: Isotope fractionation of atmospheric oxygen, Geochem. Int., 3, 241-253, 1959.

Wang, Y., Cheng, H., Lawrence Edwards, R., Kong, X., Shao, X., Chen, S., Wu, J., Jiang, X., Wang, X., and An, Z.: Millenial- and orbital-scale changes in the East Asian monsoon over the past 224,000 years, Nature, 451, 1090-1093, https://doi.org/10.1038/nature06692, 2008.

Wostbrock, A. G. J., and Sharp, Z., D.: Triple Oxygen Isotopes in Silica–Water and Carbonate–Water Systems, Rev. Mineral. Geochem., 86, 367-400, https://doi.org/10.2138/rmg.2021.86.11, 2021.